CrystEngComm

Cite this: *CrystEngComm*, 2012, **14**, 4210–4216

www.rsc.org/crystengcomm

PAPER

Two metal–organic frameworks with unique high-connected binodal network topologies: synthesis, structures, and catalytic properties†

Guang-Hua Cui,*[a] Cui-Hong He,[a] Cui-Huan Jiao,[a] Jian-Chen Geng[a] and Vladislav A. Blatov[b]

Received 23rd February 2012, Accepted 23rd March 2012
DOI: 10.1039/c2ce25264c

{[Cd_3(btec)(btx)$_{0.5}$(μ_3-OH)(H_2O)]·H_2O}$_n$ (**1**) and [Cu_2(btec)(btx)$_{1.5}$]$_n$ (**2**), two novel cadmium(II) and copper(II)-based high-connected metal–organic frameworks, with both 1,2,4,5-benzenetetracarboxylate (btec) and 1,4-bis(1,2,4-triazol-1-ylmethyl)benzene (btx) as mixed ligands were hydrothermally synthesized and structurally characterized. Both MOFs have three-dimensional (3D) structures, but different framework topologies and ligand linkage modes. **1** possesses an unprecedented binodal (4,12)-connected topology structure, in which the ligand btec serves as a rare dodecadentate and ordinary octadentate in two types of coordination modes. Meanwhile, **2** exhibits a binodal (4,7)-connected topological network with an enneadentate coordination geometry of the btec ligand. Both MOFs provide novel examples of designing and synthesizing novel binodal MOFs, and demonstrate that the 1,2,4,5-benzenetetracarboxylic acid ligand with rich coordination chemistry information is useful in the construction of binodal highly-connected nets. In addition, the catalytic performance of **2** has also been checked. **2** is active as a catalyst for the degradation of methyl orange.

Introduction

The rational design and assembly of metal–organic frameworks (MOFs) are currently quite topical research in both chemistry and materials science, due to their fascinating structural architectures and topologies, as well as their potential applications in catalysis, magnetism, gas storage and separation, nonlinear optics and so on.[1] These materials usually have a three-dimensional (3D) open framework, of these, a variety of binodal network topologies based on boracite, pyrite, rutile, and Pt_3O_4 topologies have been realized.[2] However, due to the limit of coordination numbers of metal centers and the steric hindrance of commonly used organic ligands, there is a lack of binodal high-connected structures, such as (4,7)-, (4,8)-, (4,10)-, (3,12)-, and (4,12)-connected networks.[3] Alternately, polynuclear metal clusters as secondary building units (SBUs) have been proven to be a powerful strategy in the construction of MOFs with a high-connected framework structure.[4] However, it is not easy to design and achieve a high-connected SBU, apart from trigonal prism trinuclear M_3O–$(COO)_6$ and tetranuclear zinc cluster $Zn_4O(COO)_6$ examples reported to date.[5]

1,2,4,5-Benzenetetracarboxylate (btec) has various coordination modes to metal ions, resulting from completely or partially de-protonated sites, which allows for the large diversity of framework topologies of resulting MOFs. Additionally, the strong multiple coordination of this ligand could lead to high thermal stabilities of the MOF materials.[6] On the other hand, the flexible bis(triazole) ligands are frequently introduced as secondary ligands to extend one-dimensional (1D) or two-dimensional (2D) sheets into 3D networks, or further decorate 3D networks into highly connected MOFs by displacing coordinated solvent molecules.[7] On the basis of the above considerations, two high-connected btec-metal metal–organic frameworks with 1,4-bis(1,2,4-triazol-1-ylmethyl)benzene (btx) as a secondary ligand, {[Cd_3(btec)(btx)$_{0.5}$(μ_3-OH)(H_2O)]·H_2O}$_n$ (**1**) and [Cu_2(btec)(btx)$_{1.5}$]$_n$ (**2**) have been synthesized and characterized. The relationship between unusual topological structures of resulting MOFs and coordination modes of ligands and metal clusters has been analyzed. The effective degradation of methyl orange (MO) by a Fenton-like process using **2** as a catalyst is also investigated.

Experimental section

Materials and general methods

All the solvents and reagents for synthesis were commercially available and used as received. The ligand btx was synthesized according to a literature method.[8] Elemental analysis of C, H, and N were performed on a Perkin-Elmer 240C analyzer. IR spectra were measured on an FT-IR AVATAR 360 (Nicolet) spectrophotometer with KBr pellets. Powder X-ray diffraction

[a]*College of Chemical Engineering, Hebei United University, 46 West Xinhua Road, Tangshan, 063009, Hebei, PR China. E-mail: tscghua@126.com*
[b]*Department of Chemistry, Samara State University, Ac. Pavlov St. 1, Samara, 443011, Russia*

† Electronic supplementary information (ESI) available: SBUs, the XRPD patterns and TGA plot for **1** and **2** (Fig. S1–S6). CCDC reference numbers 859630–859631. For ESI and crystallographic data in CIF or other electronic format see DOI: 10.1039/c2ce25264c

measurement was performed on a Bruker Smart 1000 CCD X-ray diffractometer using Cu-Kα radiation (λ = 0.1542 nm) in the 2θ range of 5–50° with a step size of 0.02° and a scanning rate of 10° min^{-1}.

Synthesis of {[Cd_3(btec)(btx)$_{0.5}$(μ_3-OH)(H_2O)]·H_2O}$_n$ (1) and [Cu_2(btec)(btx)$_{1.5}$]$_n$ (2)

1 was synthesized by a one-pot hydrothermal reaction: the mixture of 1,2,4,5-benzenetetracarboxylatic acid (H_4btec, 0.10 mmol, 25.4 mg), 1,4-bis(1,2,4-triazol-1-ylmethyl)benzene (btx, 0.10 mmol, 24.0 mg), $Cd(OAc)_2·2H_2O$ (0.10 mmol, 26.6 mg), and 10 mL of water was sealed in a Teflon-lined autoclave and heated to 140 °C for 3 days under autogenous pressure. Colorless block crystals of **1** were obtained after the autoclave was cooled to room temperature at a rate of 5 °C h^{-1}. The product was not homogeneous as crystals of different morphology were present. One morphology was colorless block-shaped single crystals of **1**, and it was not possible to obtain phase pure samples of **1** for chemical analysis and other measurements.

Single crystals of **2** suitable for X-ray analysis were obtained by a similar method as described for **1**, with $Cu(NO_3)_2·2.5H_2O$ instead of $Cd(OAc)_2·2H_2O$. Yields: *ca.* 56% based on Cu^{2+}. Anal. Calcd for $C_{28}H_{20}Cu_2N_9O_8$: C, 45.59; H, 2.73; N, 17.09. Found: C, 45.26; H, 2.90; N, 17.32. IR (KBr, cm^{-1}) for **2**: 3410 m, 2365 w, 1601 m, 1364 m, 1120 m, 997 m, 867 m, 821 m, 738 m, 653 m, 531 m.

Catalytic activity of 2 for the degradation of methyl orange

60 mg of **2** and 2 mL of 30% H_2O_2 were added into a 200 mL of methyl orange (MO) solution (10 mg L^{-1}), of which the pH value was adjusted to 3 with sulfuric acid (1 mol dm^{-3}), and the temperature was maintained at 318.15 K using a thermostat. At a given interval, aliquots of the reaction mixture were periodically taken and analyzed with a UV-Vis spectrophotometer at an absorption wavelength of 506 nm. This procedure was repeated in the absence of **2** as a control experiment and using equal $Cu(NO_3)_2·2.5H_2O$ as catalyst instead of **2** as the control experiment plus $Cu(NO_3)_2·2.5H_2O$.

X-ray data collection and structure determinations

X-ray single-crystal diffraction data of **1** and **2** were collected on a Bruker Smart 1000 CCD diffractometer with graphite-monochromated Mo-Kα radiation (λ = 0.71073 Å) and ω-2θ scan mode at 293 K. A semi-empirical absorption correction was applied using SADABS program.[9] The structures were solved by direct methods and refined anisotropically by full-matrix least-squares technique using Bruker's SHELXTL program package.[10] Metal atoms in each complex were located from the *E*-maps and other non-hydrogen atoms were located in successive difference Fourier syntheses and refined with anisotropic thermal parameters on F^2. The hydrogen atoms of organic ligands were generated theoretically onto the specific atoms and refined isotropically. However, the hydrogen atoms of hydroxide ion (or water molecule) were added by difference Fourier maps, and refined using a riding model. Further details for structural analysis are summarized in Table 1, and selected bond lengths and angles are listed in Table 2.

Results and discussion

Crystal structure of 1

Single-crystal X-ray diffraction analysis showed that **1** crystallized in the triclinic $P\bar{1}$ space group. The asymmetric unit of **1** contains two and a half Cd^{2+} ions, a half btx ligand, a μ_3-hydroxide anion, one btec^{4-} anion, one coordinated and one lattice water molecule. As shown in Fig. 1, there are three types of coordination environments around the Cd^{2+} ions with distorted octahedral coordination geometry. The Cd1 is surrounded by four O_{COO-} atoms from different btec^{4-} ligands, and two O atoms from different μ_3-hydroxide anions. The Cd–O bond lengths vary from 2.209(2) to 2.365(2) Å and the O–Cd–O angles range from 40.68(5) to 139.32(5)° (Table 2). Cd2 is

Table 1 Crystallographic data and structure refinement parameters for **1** and **2**.

Compound	**1**	**2**
Empirical formula	$C_{32}H_{26}Cd_5N_6O_{22}$	$C_{28}H_{20}Cu_2N_9O_8$
Molecular weight	1408.59	737.61
Crystal system	Triclinic	Monoclinic
Space group	$P\bar{1}$	$P2_1/n$
a/Å	7.4527(4)	15.0607(12)
b/Å	11.7415(6)	12.1512(10)
c/Å	12.1560(6)	16.2654(13)
α (°)	90.2620(10)	90
β (°)	103.3540(10)	113.3370(10)
γ (°)	103.3080(10)	90
Volume/Å^3	1005.29(9)	2733.1(4)
Z	1	4
D_c/Mg m^{-3}	2.327	1.793
F(000)	676	1492
Range of *h*, *k*, *l*	$-8 \leqslant h \leqslant 8$; $-13 \leqslant k \leqslant 13$; $-14 \leqslant l \leqslant 14$	$-19 \leqslant h \leqslant 19$; $-15 \leqslant k \leqslant 15$; $-21 \leqslant l \leqslant 21$
Reflections collected/unique	7679/3517	24 722/6240
R(int)	0.0163	0.0716
Goodness-of-fit on F^2	1.051	0.983
Final *R* indices [$I > 2\sigma(I)$]	R_1 = 0.0203, wR_2 = 0.0536	R_1 = 0.0428, wR_2 = 0.0934
R indices (all data)	R_1 = 0.0221, wR_2 = 0.0546	R_1 = 0.0830, wR_2 = 0.1099
$\Delta_{\rho max}/\Delta_{\rho min}$/e Å^{-3}	0.984/−0.585	0.561/−0.637

Table 2 Crystallographic data and structure refinement parameters for **1** and **2**.[a]

1			
Cd1–O6	2.224(2)	Cd1–O10B	2.270(2)
Cd1–O2	2.365(2)	Cd2–O6	2.209(2)
Cd2–O7	2.505(3)	Cd2–N3	2.293(3)
Cd2–O1	2.286(2)	Cd2–O3A	2.472(2)
Cd2–O4A	2.367(2)	Cd3–O4	2.251(2)
Cd3–O9B	2.227(2)	Cd3–O5	2.289(2)
Cd3–O8	2.266(2)	Cd3–O2	2.365(2)
Cd3–O6D	2.303(2)	O6D–Cd1–O10B	84.56(8)
O6–Cd1–O10B	95.44(8)	O6–Cd1–O2	100.91(8)
O6D–Cd1–O2	79.09(8)	O10B–Cd1–O2	89.11(9)
O6–Cd2–O3A	142.51(7)	N3–Cd2–O3A	86.77(9)
O1–Cd2–O3A	83.95(9)	O9B–Cd3–O4	164.24(10)
O4A–Cd2–O3A	53.48(8)	O4–Cd3–O8	96.87(8)
O9B–Cd3–O8	97.91(10)	O4–Cd3–O5	89.64(9)
O9B–Cd3–O5	85.17(10)	O4–Cd3–O6D	92.62(8)
2			
Cu1–O4A	1.939(2)	Cu1–O1	1.960(2)
Cu1–N1	1.973(3)	Cu1–O7	1.976(2)
Cu1–O2	2.593(3)	Cu1–O5	2.447(3)
Cu2–O8	1.953(2)	Cu2–N6	1.961(3)
Cu2–O5	1.971(2)	Cu2–N7	1.995(3)
Cu2–O6	2.545(3)	Cu2–O1	2.781(3)
O4A–Cu1–O1	88.33(10)	O4A–Cu1–N1	93.97(11)
O1–Cu1–N1	171.60(11)	O4A–Cu1–O7	170.10(10)
O1–Cu1–O7	92.96(10)	N1–Cu1–O7	86.16(10)
O5–Cu1–O7	82.10(9)	O5–Cu1–N1	93.65(10)
O5–Cu1–O4A	88.02(10)	O1–Cu2–O5	84.57(9)
O1–Cu2–O6	139.70(8)	O1–Cu2–O8	83.24(9)
O1–Cu2–N6	81.22(10)	O1–Cu2–N7	118.41(10)

[a] Symmetry codes for **1**: A: $x + 1, y, z$; B: $-x + 1, -y + 1, -z + 1$; C: $x - 1, y, z$; D: $-x, -y + 1, -z + 1$; for **2**: A: $-x + 2, -y, -z + 1$.

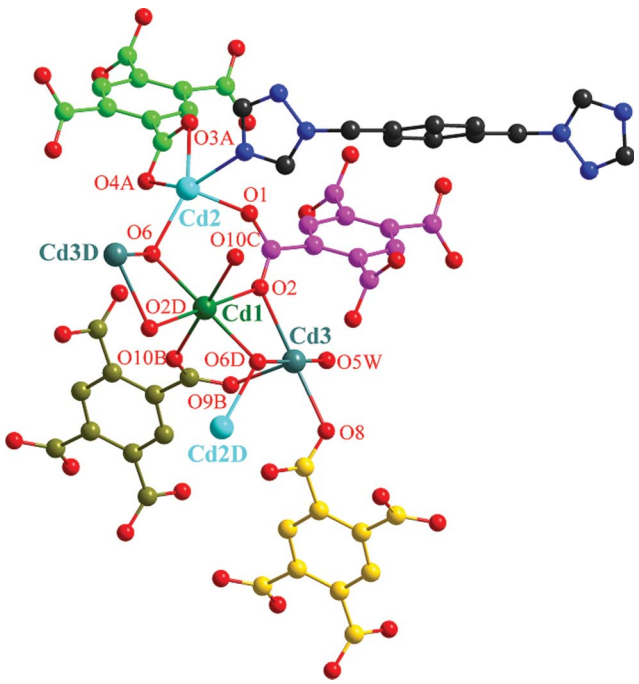

Fig. 1 The coordination environment around Cd(II) center in **1**, all hydrogen atoms were omitted for clarity, Symmetry transformations used to generate equivalent atoms: A: $x + 1, y, z$; B: $-x + 1, -y + 1, -z + 1$; D: $-x, -y + 1, -z + 1$; C: $x - 1, y, z$.

coordinated by four O_{COO-} atoms from three individual $btec^{4-}$ ligand, one O atom from the μ_3-hydroxide anion and one N atom from one btx ligand, with the Cd–O bond lengths being 2.227(2)–2.472(2) Å and the bond length Cd–N = 2.293(3) Å, the O–Cd–O angles being 83.60(10)–162.16(9)° and the O–Cd–N angles being 81.83(10)–130.68(9)° (Table 2). While the Cd3 is defined by four O_{COO-} atoms from three different $btec^{4-}$ ligands, one O atom from the μ_3-hydroxide anion and one O atom from the coordinated water molecule. The Cd–O lengths are in the range of 2.019(2)–2.276(2) Å, the O–Cd–O angles are in the range of 39.00(5)–177.20(8)°.

The rigid carboxyl groups of $btec^{4-}$ ligands are fully deprotonated and take two different kinds of coordination modes. One has a rare dodecadentate coordination, as a μ_8-$\eta^3,\eta^3,\eta^3,\eta^3$ (Scheme 1a) linker to connect eight Cd^{2+} ions. The dihedral angles between the carboxylic groups and the aromatic ring are 54.67 and 59.51°, respectively. To the best of our knowledge, this is the second observed case of a dodecadentate coordination of this ligand.[11] Another has an octadentate bridging mode and also links eight Cd^{2+} ions, and each carboxyl group adopts a μ_2-η^1,η^1 coordination mode (Scheme 1b), with the dihedral angles between the carboxylic groups and the aromatic ring of 32.65 and 62.58°, respectively.

It is noteworthy that two and a half crystallographically independent Cd^{2+} centers are connected by two μ_3-hydroxyl oxygen (O6) atoms forming a $[Cd_5(COO)_8(OH)_2]$ SBU (Fig. S1†), in which Cd1 and its neighboring Cd3 and Cd3D (symmetry code D: $-x, -y + 1, -z + 1$) are linked together through two μ_3-O and two μ_2-O atoms of two $btec^{4-}$ ligands to form an edge-sharing metallic dimer with a Cd1···Cd3 distance of about 3.4765(3) Å. The $btec^{4-}$ ligands connect *trans*-teeter-board-like Cd(II) pentameric SBUs to give a 2D layer with a **sql** tetragonal plane. These 2D layers are further cross-linked by two types of $btec^{4-}$ ligands to build a 3D framework.

The two kinds of $btec^{4-}$ ligands can been simplified as topologically equivalent 4-connected nodes, and each $[Cd_5(COO)_8(OH)_2]$ SBU is linked by eight $btec^{4-}$ ligands acting as a 8-connected node, thus, a (4,8)-connected 3D framework is formed solely by $btec^{4-}$ ligands, which is (12 examples of MOFs are known)[17] rare **scu** topology comprising octahedral and cuboctahedral cages with the Schäfli symbol of $\{4^{16}.6^{12}\}\{4^4.6^2\}$ (Fig. 2). In addition, the nitrogen atoms of the μ_2-btx bridge ligands independently further link the $[Cd_5(COO)_8(OH)_2]$ SBUs on the diagonal positions. Thus, the btec anions ligands are simplified as 4-connected nodes, and each $[Cd_5(COO)_8(OH)_2]$ SBU is linked by eight $btec^{4-}$ anion ligands and four btx ligands to act as a 12-connected node to give a (4,12)-connected network, a point symbol of $\{3^2.4^2.5^2\}_2\{3^8.4^{20}.5^{26}.6^{12}\}$ (Fig. 3). The resulting (4,12)-connected topology is a rare binodal-connected net, and has been deposited in the TOPOS database (http://www.topos.samsu.ru) as cgh1. To the best of our knowledge, only one with such connected topology has been reported lately, which is the first ionothermal case of heterometallic metal halide inorganic materials: $[CuPb_2I_2Br(OH)_2]$ with 12-connected $[Pb_4(OH)_4]$ SBUs.[12] Meanwhile here the 3D MOF is constructed by the 12-connected $[Cd_5(COO)_8(OH)_2]$ SBUs. The net in **1** provides a novel example of designing and synthesizing a novel binodal MOF and demonstrates that the 1,2,4,5-benzenetetracarboxylic acid ligand is effective in the formation of binodal highly-connected nets.

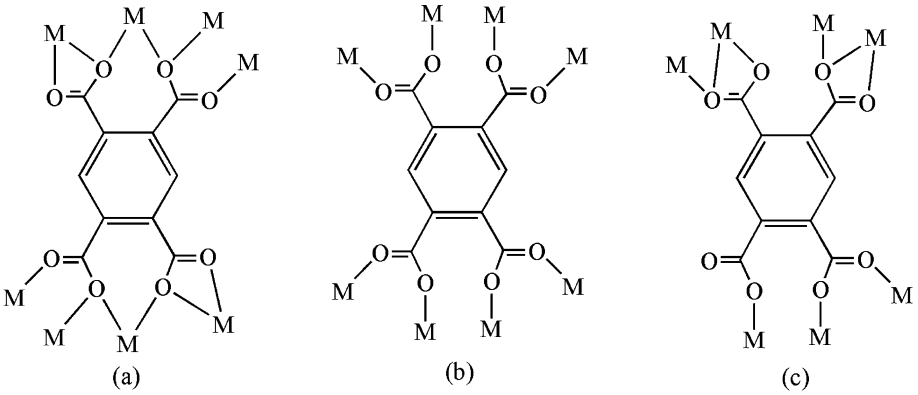

Scheme 1 The coordination modes of the $btec^{4-}$ ligands: (a) dodecadentate and (b) octadentate in **1**, (c) enneadentate in **2**.

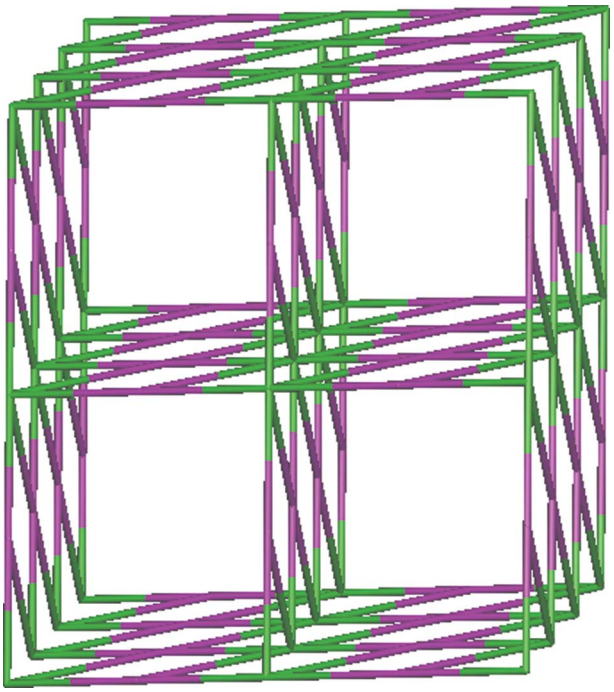

Fig. 2 A (4,8)-connected network with **scu** topology constructed by only $btec^{4-}$ ligands in **1**.

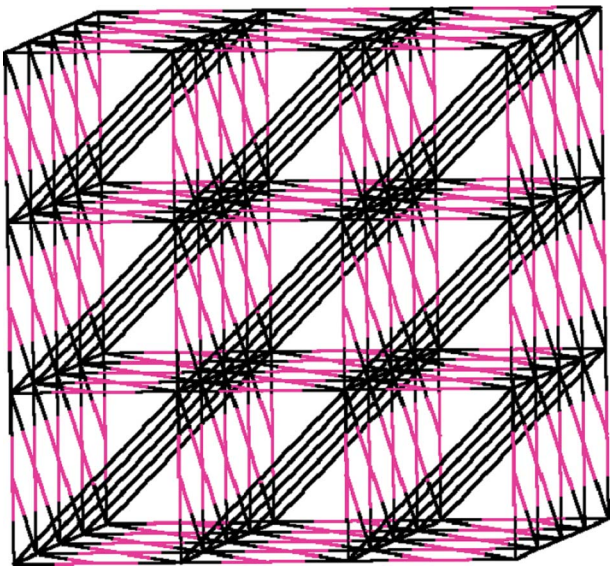

Fig. 3 A (4,12)-connected topological network of **1**.

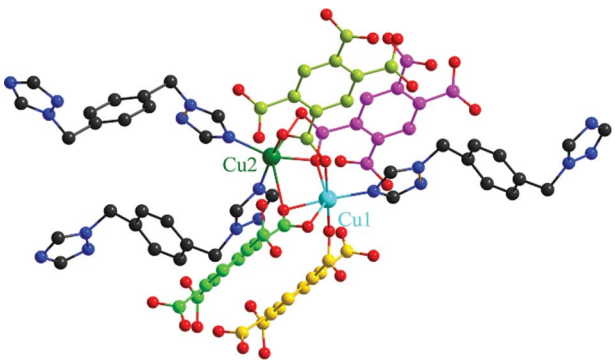

Fig. 4 The coordination environment around Cu(II) centers in **2**, all hydrogen atoms were omitted for clarity.

Crystal structure of 2

2 crystallized in the monoclinic space group $P2_1/n$. The asymmetric unit of **2** contains two Cu^{II} ions, one and a half btx ligands, and one $btec^{4-}$ anion. As illustrated in Fig. 4, Cu1 is coordinated by five O atoms from four distinct $btec^{4-}$ ligands and one btx N atom to give the CuO_5N distorted octahedral geometry; Cu2 shows the CuO_4N_2 octahedral geometry completed by two btx N atoms and four O atoms of three symmetry-related btec tetra-anions ligands. The Cu–O/N coordination bond lengths are in the normal distances (range 1.939(2)–1.995(3) Å), except for Cu1–O2 = 2.593(3) Å, Cu1–O5 = 2.447(3) Å, Cu2–O6 = 2.545(3) Å, Cu2–O1 = 2.781(3) Å (Table 2). Obviously, the bond lengths of Cu1–O2, Cu1–O5, Cu2–O6, and Cu2–O1 are longer than the normal range of the Cu–O bond, and are suggested to be non-negligible weak interactions between the metal centre and the oxygen atoms.[13,7a] These weak interactions may play an important role in fixing the metal centers in a definite coordination geometry in **2**. The two crystallographically independent Cu^{II} ions are linked together by two μ_2-O atoms of carboxylate O atoms from different $btec^{4-}$ anions to form an edge-sharing copper dimer ($[Cu_2(COO)_4]$) with a Cu1···Cu2 distance of 3.228(8) Å (Fig. S2†).

Interestingly, the fully-deprotonated $btec^{4-}$ anions coordinate with the unprecedented μ_7-$\eta^3,\eta^3,\eta^2,\eta^1$ coordination mode (Scheme 1c) by connecting seven Cu^{2+} ions and the dihedral angles between the carboxylic groups and the aromatic ring are 35.75, 53.51, 60.54, 47.94°. To the best of our knowledge, this is the first case of enneadentate coordination of $btec^{4-}$ anion. Each $btec^{4-}$ bridges seven Cu^{II} ions to form a 2D rhomboid sheet $[Cu_2(btec)]_n$. If the copper dimer ($[Cu_2(COO)_4]$) SBUs and $btec^{4-}$ organic ligands are viewed as a seven and four-connected nodes, respectively, then this MOF presents a form of 2D layer with **sql** tetragonal plane (Fig. 5). These 2D layers are further linked by two types of btx ligands acting as bridging pillars to build a 3D pillared-layer network. It is worth mentioning that adjacent layers are pillared by three btx spacers, which is different from some unipole frameworks.

Thus a significant feature of **2** is the resulting unusual binodal (4,7)-connected topology based on $[Cu_2(COO)_4]$ SBUs. Each $btec^{4-}$ is linked to four equivalent $[Cu_2(COO)_4]$ SBUs to act as a 4-connected node, and each $[Cu_2(COO)_4]$ SBUs is bound by four $btec^{4-}$ ligands and three btx ligands to act as a 7-connected node, thus, a (4,7)-connected network is generated with a point symbol of $\{4^4.6^2\}\{4^6.6^{13}.8^2\}$ (Fig. 6). The resulting (4,7)-connected topology is an unprecedented binodal-connected net based on 1,2,4,5-benzenetetracarboxylic acid ligand, and has been deposited in the TOPOS database (http://www.topos.samsu.ru) as cgh2. To the best of our knowledge, this is first example of MOF with such a connected topology.

XRPD and thermal properties

Bulk samples of **1** and **2** were characterized *via* X-ray powder diffraction (XRPD) at room temperature. The sample batch of **1** is not homogeneous as seen in the powder X-ray diffraction patterns in the ESI (Fig. S3†). The decomposition of **1** is probably due to either solvent evaporation or structural rearrangement, as earlier observed in zinc coordination polymers.[14] The simulated and experimental XRPD patterns of **2** are shown in Fig. S4,† the peak positions match well with each other, indicating the phase purity of the product. The differences in intensity may be due to the preferred orientation of the powder sample.

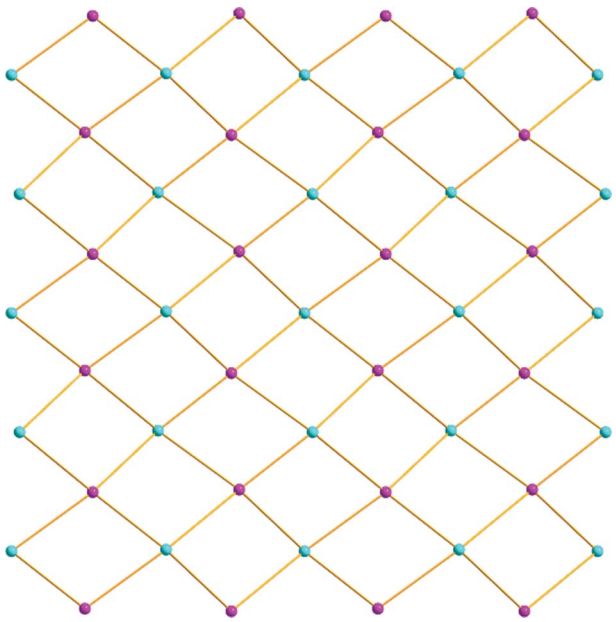

Fig. 5 2D layer with **sql** tetragonal plane constructed by only $btec^{4-}$ ligands viewed along the *a* axis in **2**. The cyan ball represents copper dimer ($[Cu_2(COO)_4]$) SBUs and purple ball represent $btec^{4-}$ organic ligands.

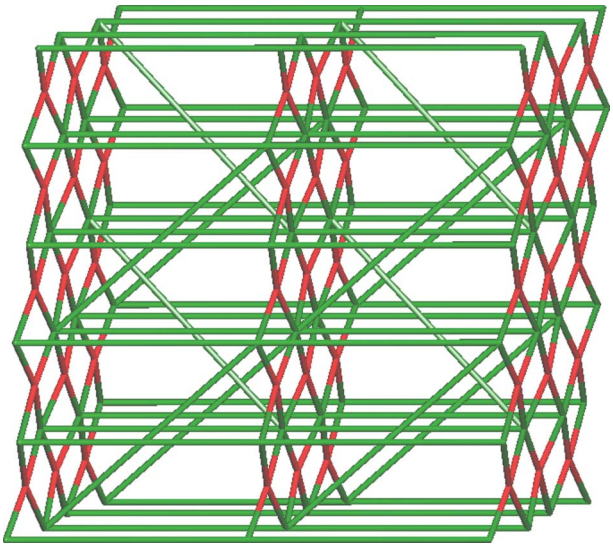

Fig. 6 The (4,7)-connected topological network of **2**.

The thermal properties of two compounds have been analysed by TG under N_2, and are shown in Fig. S5–S6.† The decomposition of **1** can be divided into two steps from the TG curve. The first mass loss of 7.03% between 119.8 and 136 °C corresponds to release of the coordination water, coordination hydroxyl and lattice-water molecules (calcd 7.53%). The second mass loss of 49.67% from 336.4 to 448.9 °C is ascribed to the loss of btx and btec ligands (calcd 52.54%). The residual CdO has a mass of 43.3% (calcd 45.58%). **2** has two weight loss processes. Initially, **2** is stable up to 264.5 °C and then with further heating to 337.2 °C, a gradual weight loss occurs, which is due to loss of the btec ligand (obsd 32.16; calcd 33.89%). Secondly, a weight loss of 47.62% is observed from 347.9 to 423.3 °C, assigned to the loss of btx (calcd 48.81%). The residue corresponds to the formation of CuO (obsd 20.22; calcd 21.57%).

Catalytic activity of 2 for the degradation of methyl orange

To date, most attention has been focused on the Fenton and Fenton-like reaction to oxidize contaminants of concern such azo dyes, and is largely dependent on transition metal based catalysts. In particular, this technique has the potential to completely mineralize organic compounds.[15] The degradation experiment of MO was tracked by visible spectroscopy and the results are depicted in Fig. 7 (the vertical axis shows the percentage of MO degradation rate at time *t*). It was found that the degradation rate of MO is up to 96.1% at the optimal conditions of 95 min in the present of **2**. However, when the research was conducted in the control experiment and control

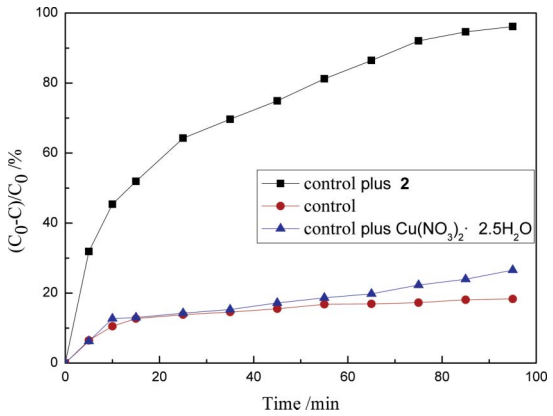

Fig. 7 The experiments of the degradation of methyl orange under: (a) control plus **2**; (b) control; (c) control plus $Cu(NO_3)_2{\cdot}2.5H_2O$.

experiment plus $Cu(NO_3)_2{\cdot}2.5H_2O$, the degradation efficiency of the reaction was reduced to 18.31% and 26.56% in 95 min, respectively. Clearly, **2** is an effective catalyst for the wet hydrogen peroxide catalytic oxidation of MO by hydroxyl radicals in the Fenton-like process.

The use of a solid catalyst was shown to increase performance and lower operational costs.[15b] H_2O_2 is the precursor of hydroxyl radicals, which are effective and highly active oxidizing species. Generation of hydroxyl radicals occurs either using UV radiation or through the use of a catalyst (iron or copper ions) by the well-known Fenton type mechanism, where Fe^{2+} or Cu^{+} reacts with H_2O_2 to generate hydroxyl radicals. Due to the presence of a reaction cycle, Fe^{3+} and Cu^{2+} ions could also be used as Fenton catalysts. It is possible to represent the MO degradation by the following simplified schema (Scheme 2). A reduction–oxidation cycle of Cu(II)–Cu(I) generating $^{\bullet}OH$ radicals seems to be the possible route for the Fenton-like degradation of MO.[15] **2** shows catalytic activity not only due to Cu(II) metal center, but also the directionality of copper–ligand interaction and the angles defined by the multipodal linker, which generate micro cavities/channels that can be accessed from the exterior allowing mass transfer and the incorporation of substrates inside the crystal.[16]

In summary, two high-connected 3D MOFs have been hydrothermally synthesized, structurally characterized, and catalytic properties checked. The successful construction of the two MOFs with novel topological networks reveals that sensibly tuning the coordination modes of multifunctional 1,2,4,5-benzenetetracarboxylate ligand could be an effective method to generate different SBUs, thereby tuning the structural formation of resulting compounds. Meanwhile, the btx ligand as a good candidate of secondary ligand not only can extend structural dimension of its complexes through the pillared–layered method but also can modify the structures to obtain high-connected frameworks. **2** displays high catalytic activity in the Fenton-like process to degrade MO, implying its application potential as a solid catalyst. Further work is focusing on the exploration of other multi-carboxylate-based ligands for the construction of novel MOFs with unique structural topologies and associated properties.

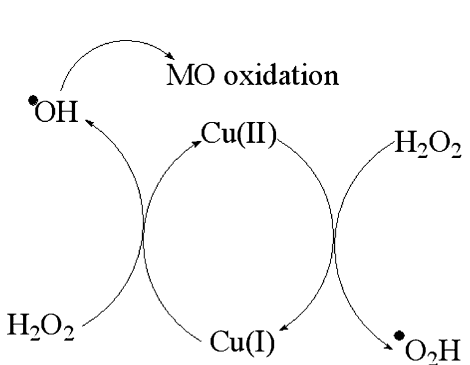

Scheme 2 Schematic representation of catalysis reaction of **2**.

Acknowledgements

This work was supported by Hebei United University. We would also like to thank Prof. Jian-Rong Li of Beijing University of Technology for his valuable discussion.

References

1 (*a*) A. D. Boisselier and E. C. Ornelas, *Chem. Rev.*, 2010, **110**, 1857–1959; (*b*) J.-R. Li, J. Sculley and H.-C. Zhou, *Chem. Rev.*, 2012, **112**, 869–932; (*c*) J. Zhang, L. Wojtas, R. W. Larsen, M. Eddaoudi and M. J. Zaworotko, *J. Am. Chem. Soc.*, 2009, **131**, 17040–17041; (*d*) M. H. Zeng, W. X. Zhang, X. Z. Sun and X. M. Chen, *Angew. Chem., Int. Ed.*, 2005, **44**, 3079–3082; (*e*) J.-R. Li, T. Daren and H.-C. Zhou, *J. Am. Chem. Soc.*, 2009, **131**, 6368–6369; (*f*) R. Feng, F. L. Jiang, L. Chen, C. F. Yan, M. Y. Wu and M. C. Hong, *Chem. Commun.*, 2009, 5296–5298; (*g*) X. H. Bu, M. L. Tong, H. C. Chang, S. Kitagawa and S. R. Batten, *Angew. Chem., Int. Ed.*, 2004, **43**, 192–195; (*h*) R. F. Song, Y. B. Xie, J. R. Li and X. H. Bu, *Dalton Trans.*, 2003, 4742–4748; (*i*) J.-R. Li, Y. Ma, M. C. McCarthy, J. Sculley, J. Yu, H.-K. Jeong, P. B. Balbuena and H.-C. Zhou, *Coord. Chem. Rev.*, 2011, **255**, 1791–1823; (*j*) J. Lu, D. R. Turner, L. P. Harding, L. T. Byrne, M. V. Baker and S. R Batten, *J. Am. Chem. Soc.*, 2009, **131**, 10372–10373; (*k*) T. L. Hu, J. R. Li, C. S. Liu, X. S. Shi, J. N. Zhou, X. H. Bu and J. Ribas, *Inorg. Chem.*, 2006, **45**, 162–173; (*l*) J.-R. Li, Q. Yu, Y. Tao, X.-H. Bu, J. Ribas and S. R. Batten, *Chem. Commun.*, 2007, 2290–2292; (*m*) G. H. Cui, J. R. Li, J. L. Tian, X. H. Bu and S. R. Batten, *Cryst. Growth Des.*, 2005, **5**, 1775–1778.

2 (*a*) B. F. Abrahams, S. R. Batten, H. Hamit, B. F. Hoskins and R. Robson, *Angew. Chem., Int. Ed. Engl.*, 1996, **35**, 1690–1692; (*b*) H. K. Chae, J. Kim, O. D. Friedrichs, M. O'Keeffe and O. M. Yaghi, *Angew. Chem., Int. Ed.*, 2003, **42**, 3907–3909; (*c*) S. R. Batten, B. F. Hoskins and R. Robson, *J. Chem. Soc., Chem. Commun.*, 1991, 445–447; (*d*) B. L. Chen, M. Eddaoudi, S. T. Hyde, M. O'Keeffe and O. M. Yaghi, *Science*, 2001, **291**, 1021–1023.

3 (*a*) Z. J. Lin, T. F. Liu, X. L. Zhao, J. Lu and R. Cao, *Cryst. Growth Des.*, 2011, **11**, 4284–4287; (*b*) X. Li, H. L. Sun, X. S. Wu, X. Qiu and M. Du, *Inorg. Chem.*, 2010, **49**, 1865–1871; (*c*) S. Q. Ma and H. C. Zhou, *J. Am. Chem. Soc.*, 2006, **128**, 11734–11735; (*d*) R. Q. Zou, R. Q. Zhong, M. Du, T. Kiyobayashi and Q. Xu, *Chem. Commun.*, 2007, 2467–2469; (*e*) Y. Q. Lan, S.L. Li, Y. G. Li, Z. M. Su, K. Z. Shao and X. L Wang, *CrystEngComm*, 2008, **10**, 1129–1131; (*f*) C. Y. Wang, Z. M. Wilseck, R. M. Supkowskic and R. L. LaDuca, *CrystEngComm*, 2011, **13**, 1391–1399; (*g*) K. M. Blake, J. S. Lucas and R. L. LaDuca, *Cryst. Growth Des.*, 2011, **11**, 1287–1293.

4 (*a*) J. Kim, B. Chen, T. M. Reineke, H. Li, M. Eddaoudi, D. B. Moler, M. O'Keeffe and O. M.Yaghi, *J. Am. Chem. Soc.*, 2001, **123**, 8239–8247; (*b*) J. R. Li, Y. Tao, Q. Yu and X. H. Bu, *Chem. Commun.*, 2007, 1527–1529; (*c*) L. Hou, W. X. Zhang, J. P. Zhang, W. Xue, Y. B. Zhang and X. M. Chen, *Chem. Commun.*, 2010, **46**, 6311–6313; (*d*) Q. G. Zhai, C. Z. Lu, X. Y. Wu and S. R. Batten, *Cryst. Growth Des.*, 2007, **7**, 2332–2342.

5 Q. Chen, J. B. Lin, W. Xue, M. H. Zeng and X. M. Chen, *Inorg. Chem.*, 2011, **50**, 2321–2328.

6 (*a*) A. Majumder, V. Gramlich, G. M. Rosair, S. R. Batten, J. D. Masuda, J. Ribas, J. P. Sutter, C. Desplanches and S. Mitra, *Cryst.*

Growth Des., 2006, **6**, 2355–2368; (*b*) O. Fabelo, J. Pasan, L. Canadillas-Delgado, F. S. Delgado, F. Lloret, M. Julve and C. Ruiz-Perez, *Inorg. Chem.*, 2008, **47**, 8053–8058; (*c*) D. Q. Chu, J. Q. Xu, L. M. Duan, T. G. Wang, A. Q. Tang and L. Ye, *Eur. J. Inorg. Chem.*, 2001, 1135–1137; (*d*) M. D. Stephenson and M. J. Hardie, *Cryst. Growth Des.*, 2006, **6**, 423–432; (*e*) A. Majumder, V. Gramlich, G. M. Rosair, S. R. Batten, J. D. Masuda, M. S. E. Fallah, J. Ribas, J. P. Sutter, C. Desplanches and S. Mitra, *Cryst. Growth Des.*, 2006, **6**, 2355–2368; (*f*) P. Wang, C. N. Moorefield, M. Panzer and G. R. Newkome, *Chem. Commun.*, 2005, 465–467; (*g*) J. Yang, J. F. Ma, Y. Y. Liu, S.-L. Li and G. L. Zheng, *Eur. J. Inorg. Chem.*, 2005, 2174–2180.

7 (*a*) C. Ren, L. Hou, B. Liu, G. P. Yang, Y. Y. Wang and Q. Z. Shi, *Dalton Trans.*, 2011, **40**, 793–804; (*b*) Y. Mu, J. Fu, Y. Song, Z. Li, H. W. Hou and Y. T. Fan, *Cryst. Growth Des.*, 2011, **11**, 2183–2193.

8 B. F. Hoskins, R. Robson and D. A. Slizys, *J. Am. Chem. Soc.*, 1997, **119**, 2952–2953.

9 G. M. Sheldrick, *SADABS, Program for area detector adsorption correction*, Institute for Inorganic Chemistry, University of Göttingen, Germany, 1996.

10 *SHELXTL 6.10*, Bruker Analytical Instrumentation, Madison, Wisconsin, USA, 2000.

11 L.M. Zhao, H. H. Li, Y. Wu, S.Y. Zhang, Z. J. Zhang, W. Shi, P. Cheng, D. Z. Liao and S. P. Yan, *Eur. J. Inorg. Chem.*, 2010, 1983–1990.

12 F. Hu, Q. G. Zhai, S. N. Li, Y. C. Jiang and M. C. Hu, *CrystEngComm*, 2011, **13**, 414–417.

13 A. Bondi, *J. Phys. Chem.*, 1964, **68**, 441–451.

14 H. F. Clausen, R. D. Poulsen, A. D. Bond, M.-A. S. Chevallier and B. B. Iversen, *J. Solid State Chem.*, 2005, **178**, 3342–3351.

15 (*a*) B. Ahmed, E. Limem, A. Abdel-Wahab and B. Nasr, *Ind. Eng. Chem. Res.*, 2011, **50**, 6673–6680; (*b*) A. Pintar and J. Levec, *Chem. Eng. Sci.*, 1992, **47**, 2395–2400; (*c*) C. A. Tolman, W. Tumas, S. Y. L. Lee, D. Campos, in *The Activation of Dioxygen and Homogeneous Catalytic Oxidation*, ed. D. H. R. Barton, Plenum Press, New York, 1993, 514.

16 A. Corma, H. Garcia and F. X. L. Xamena, *Chem. Rev.*, 2010, **110**, 4606–4655.

17 E. V. Alexandrov, V. A. Blatov, A. V. Kochetkova and D. M. Proserpio, *CrystEngComm*, 2011, **13**, 3947–3958.

